

Fermi National Accelerator Laboratory

FERMILAB-Pub-97/274-E

E835

**The Variable Density Gas Jet Internal Target for Experimental 835
at Fermilab**

D. Allspach et al.
The E835 Collaboration

*Fermi National Accelerator Laboratory
P.O. Box 500, Batavia, Illinois 60510*

October 1997

Submitted to *Nuclear Instruments and Methods*

Disclaimer

This report was prepared as an account of work sponsored by an agency of the United States Government. Neither the United States Government nor any agency thereof, nor any of their employees, makes any warranty, expressed or implied, or assumes any legal liability or responsibility for the accuracy, completeness, or usefulness of any information, apparatus, product, or process disclosed, or represents that its use would not infringe privately owned rights. Reference herein to any specific commercial product, process, or service by trade name, trademark, manufacturer, or otherwise, does not necessarily constitute or imply its endorsement, recommendation, or favoring by the United States Government or any agency thereof. The views and opinions of authors expressed herein do not necessarily state or reflect those of the United States Government or any agency thereof.

Distribution

Approved for public release; further dissemination unlimited.

The Variable Density Gas Jet Internal Target for Experiment 835 at Fermilab

D. Allspach, A. Hahn, C. Kendziora, and S. Pordes
Fermi National Accelerator Laboratory, Batavia, IL, USA

G. Boero, G. Garzoglio, M. Macri, M. Marinelli, M. Pallavicini, and E. Robutti
Istituto Nazionale di Fisica Nucleare e Universita di Genova, Italy

Abstract

The hydrogen Jet Target for Experiment 835 (Charmonium spectroscopy) at the Fermilab Antiproton Accumulator can provide a variable density cluster stream up to $3.2 \cdot 10^{14}$ atoms/cc in order to allow an instantaneous luminosity greater than $2 \cdot 10^{31}$ cm⁻²s⁻¹. This result can be achieved due to the helium refrigerated expansion stage which provides the cluster stream and due to the pumping and the alignment system which significantly lower the background gas. Details on the construction and the performances, measured in the laboratory and during the run, are discussed.

1. Introduction

The use of internal gas jet targets in high energy physics experiments [1] provides a source of interaction with unique characteristics. Its main feature resides in the efficient use of the particle beam coasting in the storage ring: this is most important when the beam requires a long time and high cost to be accumulated and maintained, as in the case of antiproton beams.

The main problem arising with the use of internal targets is their effect on the beam lifetime and properties (such as size and momentum). The development of stochastic cooling techniques applied to horizontal and vertical betatron oscillations and to momentum (synchrotron) oscillations led to excellent results in recent years. In particular, hydrogen jet targets were built by the Genova I.N.F.N. group for experiments R704 [2], PS202 [3], PS210 [4] at CERN and for E760 [5] at Fermilab.

The success of the E760 program led to the decision to begin a new experiment identified as E835 [6]. The antiproton beam is produced in the Fermilab Antiproton Source. A 120 GeV proton beam focused on a fixed target yields approximately one antiproton for every 10^6 protons. Roughly $8 \cdot 10^{11}$ antiprotons can be collected over a period of 24 hours. With this quantity of antiprotons circulating in the Antiproton Accumulator, the beam has a current of 80 mA. In the absence of the hydrogen gas jet stream, the antiproton beam lifetime is around 400 hours. During experimentation an interaction rate of 1.4 MHz

between the jet stream and the antiproton beam is chosen resulting in a beam lifetime of about 50 hours.

In order to maximize the amount of collectable data, the interaction rate is kept constant. While taking data with a single stack of antiprotons, the antiproton current varies from 80 mA to about 5 mA. The E835 jet target has the capability of varying the density from $1 \cdot 10^{13}$ to $3.2 \cdot 10^{14}$ atoms/cc, which provides a constant luminosity of $2 \cdot 10^{31}$ $\text{cm}^{-2}\text{s}^{-1}$ during most of the run. Those values need to be compared with a peak density of $6 \cdot 10^{13}$ atoms/cc reached for E760. At the same time, the jet should maintain the characteristics of excellent spatial definition and a low background gas level.

The upgrade program, carried out by the Fermilab Research Division and Genova I.N.F.N. section, required substantial modifications to the former E760 system. These modifications include:

- (1) Lowering the stagnation temperature of the hydrogen gas supplied at the jet source nozzle such that the density of the hydrogen jet stream is increased.
- (2) Improving the system pumping speed acting on the vacuum chamber in which the gas jet is located. This reduces the interaction rate of the antiproton beam with the background gas associated with the jet stream.
- (3) Controlling the source position in the plane normal to the jet stream and its angular position. This results in a perfect alignment of the jet stream with respect to the antiproton beam. This minimizes the quantity of gas which enter the Antiproton Accumulator, but is not directly absorbed by the sink system: this constitutes the background gas.

This paper is organized as follows. Section 2 outlines some properties of cluster jet targets and describes how they are produced through gas expansion in a properly shaped nozzle. Section 3 deals with the central point of the program upgrade, describing the differential pumping system of the machine and the temperature and pressure control of the gas jet system. The method used to measure jet flux and speed, required for determining density, is also described. Results from these measurements are used to draw conclusions on actual system performance.

2. The jet source

The gas jet used for the E760-E835 target belongs to the so-called "cluster jet" type, in which the core of the jet is made up of micro droplets, or "clusters" of condensed matter (in our case hydrogen).

The cluster jets are produced through expansion of a gas through a convergent-divergent nozzle in condition of high pressure and low temperature (see Fig. 1). The sudden decrease in pressure and temperature caused by expansion sets the gas in a supersaturated state and favors the formation and growth of clusters whose size may vary from 10^7 to 10^8 molecules [7].

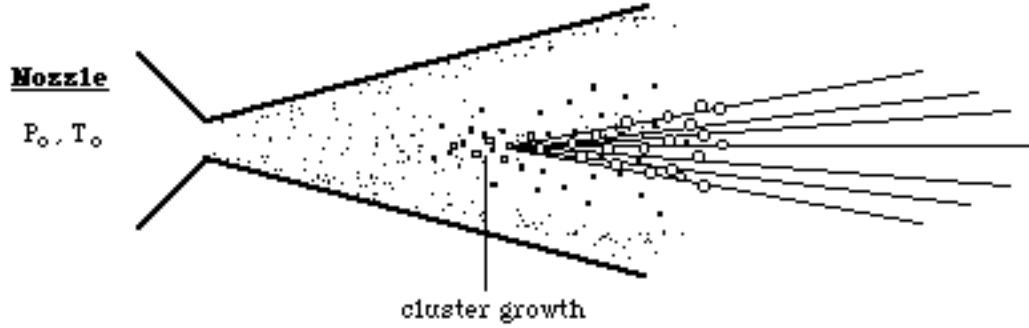


Fig. 1: Condensation and formation of the cluster stream, due to the adiabatic expansion of the gas inside the trumpet shaped nozzle.

Despite the complexity of the condensation process, a qualitative treatment is possible using thermodynamic equations for isentropic expansion [8]:

$$T = T_0 \left(1 + \frac{\gamma - 1}{2} M^2 \right)^{-1}$$

$$v = M \sqrt{\frac{\gamma R T_0}{m} \left(1 + \frac{\gamma - 1}{2} M^2 \right)^{-\frac{1}{2}}}$$

$$P = P_0 \left(1 + \frac{\gamma - 1}{2} M^2 \right)^{-\frac{\gamma}{\gamma - 1}}$$

$$\rho = \rho_0 \left(1 + \frac{\gamma - 1}{2} M^2 \right)^{-\frac{1}{\gamma - 1}}$$

where P_0 , T_0 and ρ_0 are the initial gas pressure, temperature and density, defined by the nozzle status; P , T and ρ are the gas conditions during the expansion; M is the Mach number and $\gamma = c_p/c_v$.

From the previous formulae it can be seen that for suitable values of P_0 and T_0 the point representing the state of the gas in the P - T diagram can move into the liquid side of the saturation curve (Fig. 2 [7]), thus starting the condensation process.

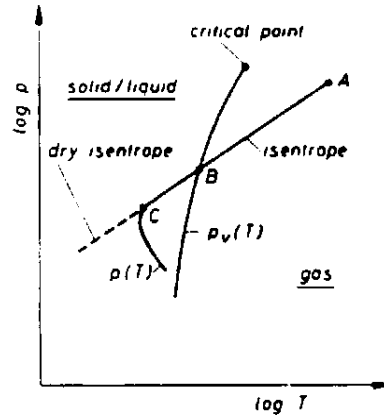


Fig. 2: Isentropic curve for a particular expansion and transition curve on the pressure and temperature plane

The clusters constitute the core of the gas flow exiting the nozzle. They show the remarkable property of having a very narrow speed distribution, which cause them to form a high density jet with directional spread within a small cone (few degrees) around its axis (for the experiment we use only a fraction of this angular range; the remaining gas needs to be pumped out). This feature can be enhanced by choosing an appropriate shape for the nozzle. Best results have been achieved with trumpet-shaped nozzles: this is therefore the shape we chose as well. Our nozzle has an opening angle of 3.5° , a divergent length of 8 mm and a throat diameter of $37 \mu\text{m}$.

The working points for the nozzle pressure (P) and temperature (T) are based on the following factors. It is sensible to expect that, for a given pressure, the core of the cluster stream becomes denser as the temperature decreases. Therefore, to increase the gas jet density, with the minimum background, one should increase the pressure and decrease the temperature, but avoid the phase transition. The saturation curve is the upper border which limits the pressure for a given temperature. This border defines the curve to be followed to achieve the higher jet densities (Fig. 12).

To be able to use the jet as a target inside a storage ring, one has to isolate the cluster jet stream from the remaining ("background") gas exiting the nozzle. The primary reason is to prevent large quantities of gas from entering the accumulator pipe, where a high vacuum must be kept at all times. This is achieved by making use of a differential pumping system (Fig. 3), with the jet crossing a series of chambers which are independently evacuated.

The dimensions of the jet at the interaction region (7 mm) is set from the skimmer between the second and the third chamber (see "second skimmer" in Fig. 6), which, having an aperture diameter of 4.3 mm, selects the dense core of the jet (1.5°). The first skimmer eliminates most of the gas exiting the nozzle, selecting a jet angle of 3° ; it has a diameter of 1.4 mm. It has been possible to minimize the conductance of this skimmer, and the

background gas as well, by the use of the nozzle alignment system: horizontal, vertical and angular movements are allowed. An ion gauge, mounted on the geometrical axis of the vacuum chambers and located in the last recovery chamber, helps the alignment of the jet. In table 1 [9] is written the conductance of each skimmer and diaphragm between the chambers.

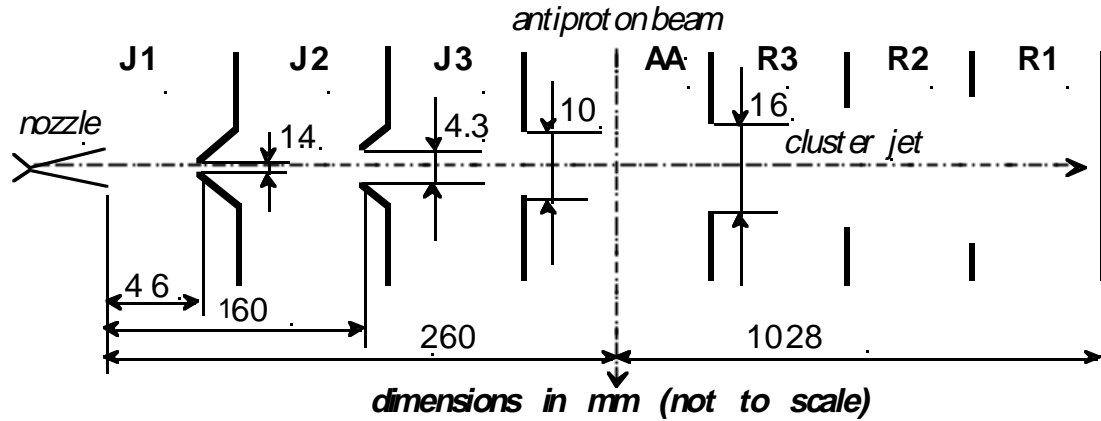


Fig. 3: Schematic of the seven chamber differential pumping system.

3. Gas Jet Setup

Pumping system.

The configuration of the *pumping system* is the result of a trade-off between the need to have high pumping speeds and the space limitations imposed on the Jet Target by the presence of the E835 detector just downstream of the interaction point (Fig. 4).

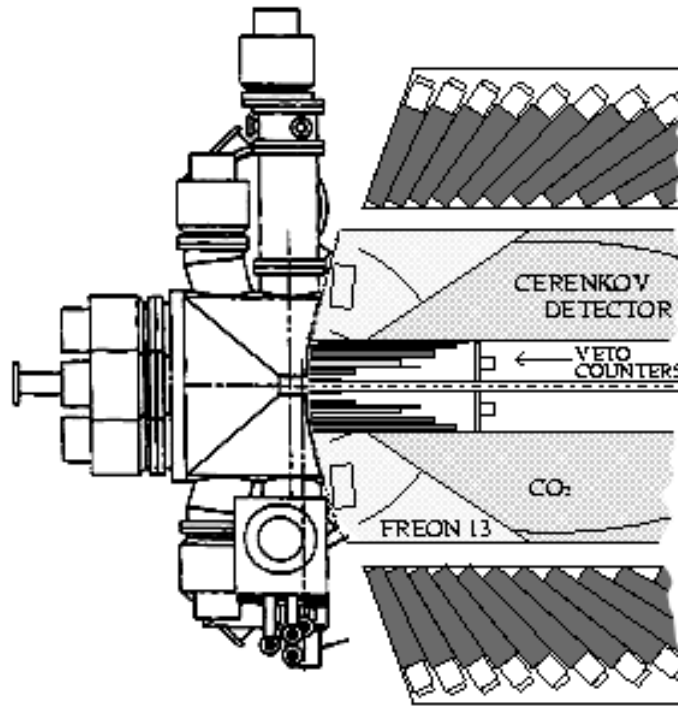


Fig. 4: The detector of E835 in the region next to the jet target.

Ten turbomolecular pumps (TMP's) are installed directly onto the chambers. Eight of these have a capacity of 1000 L/s and two are rated for 3500 L/s. The actual pumping speed in each chamber has been measured by the use of a calibrated hydrogen flow (see Table 1)[9]. The conductance of the skimmer and diaphragms between chambers have been measured with the same method as well.

Pumping Speed for N₂	Pumping Speed for H₂	Conductance for H₂
$S_{J1} = 1180$ lit/sec	$S_{J1} = 1450$ lit/sec	
	$S_{J2} = 650$ lit/sec	$C_{J1-J2} < 2$ lit/sec
$S_{J3} = 480$ lit/sec	$S_{J3} = 660$ lit/sec	$C_{J2-J3} = 6$ lit/sec
$S_{AA} = 115$ lit/sec	$S_{AA} = 520$ lit/sec	$C_{J3-AA} = 25$ lit/sec
$S_{AA1} = 520$ lit/sec	$S_{R3} = 700$ lit/sec	$C_{AA-R3} = 40$ lit/sec
	$S_{R2} = 740$ lit/sec	$C_{R3-R2} = 100$ lit/sec
$S_{R1} = 1130$ lit/sec	$S_{R1} = 2350$ lit/sec	$C_{R2-R1} = 150$ lit/sec

Table 1. Measured values of the pumping speed (N₂ and H₂) and conductance (H₂). These pumping speeds are measured for pressures below $5 \cdot 10^{-4}$ torr. The AA pumping speed during the test was limited by the system used for the cluster-jet shape measurements.

Due to the low compression ratio of the turbomolecular pumps for hydrogen, the pumping system has been designed to avoid limiting the pressure in the high vacuum zone of each pump due to the rough vacuum pressure. To achieve this result, two additional turbomolecular pumps are used as booster pumps downstream of the pumps on the J2, J3, AA1, AA2, R1, R2 and R3 chambers. Also included are three positive displacement blowers and two roughing pumps (see Fig.5).

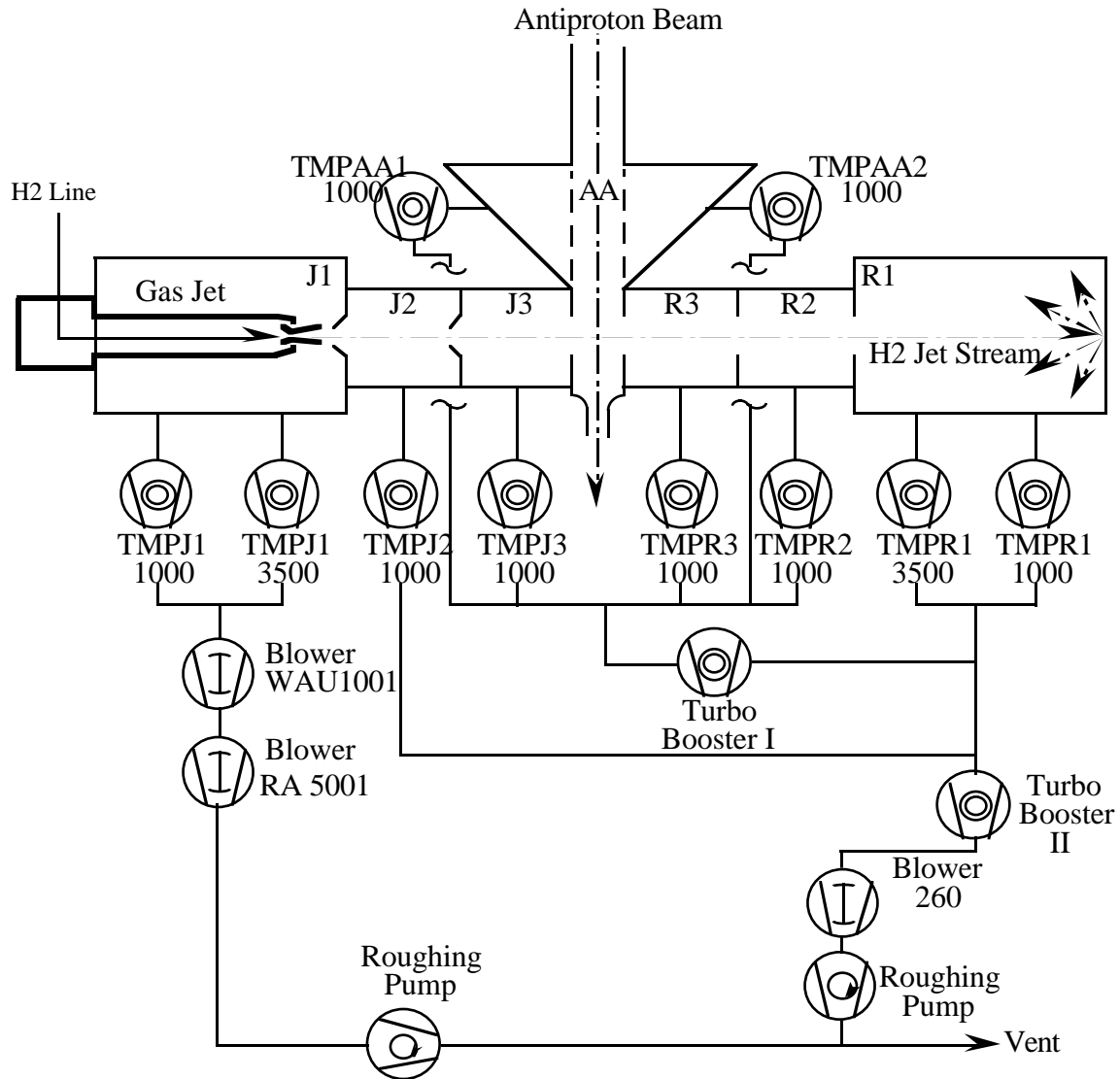


Fig. 5: The Jet Target Pumping System. The structure has been designed to prevent limitation of the chamber pressure by the compression ratio of the pumps.

Hydrogen supply line.

To control the hydrogen gas pressure at the nozzle inlet, a multiple loop controller is used. A high performance pressure transmitter provides the pressure reading to the controller. An electromagnetically operated flow control valve is then positioned by the controller in order to maintain the gas set pressure. The operating range is 3 - 120 psia with a precision of 0.5 psi.

Before entering the refrigeration system, the hydrogen gas is purified by mechanical filters and a liquid nitrogen cold trap. This is to avoid plating contaminants in the refrigerated hydrogen circuit and to prevent the small aperture of the nozzle from becoming partially or completely clogged.

Temperature control.

The nozzle through which the H_2 passes is located inside the J1 chamber (Fig. 6)[10]. The cooling is achieved by the use of a two stage helium cryocooler, commercially rated for 9W at 20K. The coldest second stage extension is thermally coupled to a copper spool through which the hydrogen gas flows: here it is cooled down to its stagnation temperature before expansion. The nozzle is kept in place by a metallic support (*nozzle holder*): this is thermally coupled to the spool by copper cables to ensure mobility of the nozzle.

All of this is enclosed in a vacuum tight structure. To reduce heat transfer by radiation from the shell walls to the nozzle and coldfinger of the cryocooler, shields cooled with liquid nitrogen are installed. The cryocooler extension (whose temperature can reach values as low as 10K), has installed another shield around it and is cooled to about 50K by the first stage of the cryocooler.

The cooling and expansion stage is located just upstream of the J1 chamber radiation shield. This shield decouples the nozzle holder from the radiation heat transfer. Furthermore, cooling the gas around the nozzle, it reduces the mean energy transferred to the cluster for scattering processes. This virtually eliminates the evaporation of H_2 molecules from the clusters.

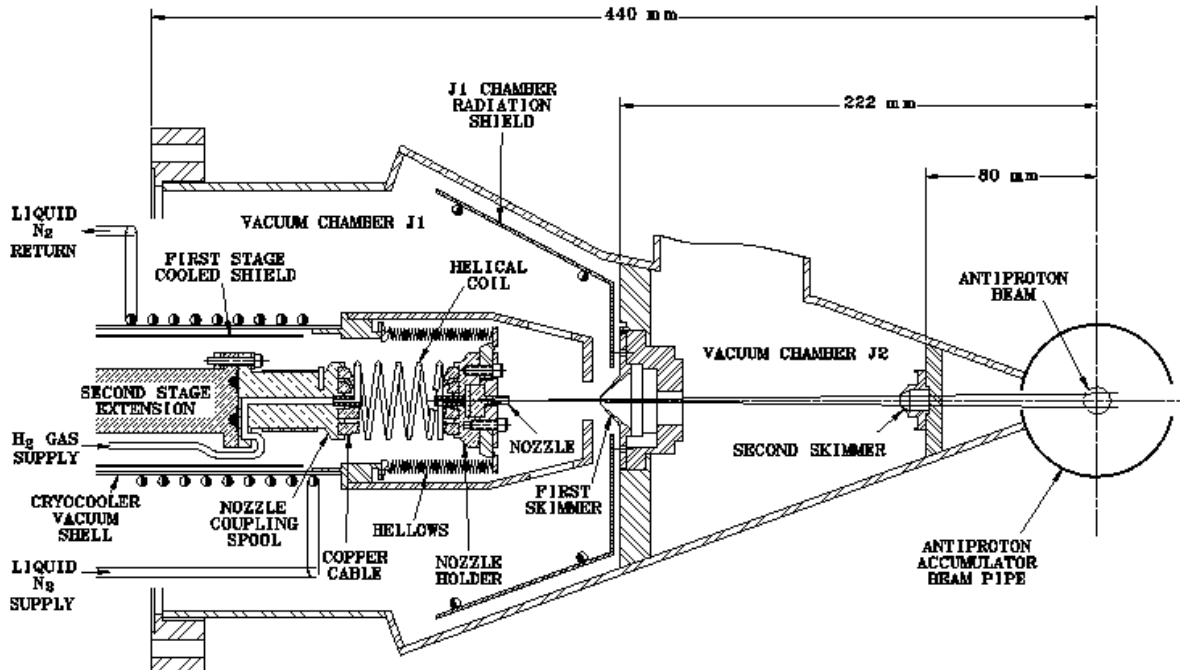


Fig. 6: Hydrogen Gas Jet components located in the J1 Vacuum Chamber

The nozzle is nearly the coldest component of the hydrogen circuit. As pointed out in section 2, the useful working temperature range of the nozzle for data taking is from 15K to 40K. The sensitivity of the temperature control in this range is better than 0.01K. The nozzle temperature is sensed with a calibrated germanium resistance thermometer located on the nozzle holder. The sensor is positioned in a cavity whose dimensions create a close sliding fit with the sensor. A vacuum grease with good thermal conductance is used to minimize the contact resistance. A 16 bit temperature controller reads the nozzle temperature and provides an analog voltage output to a heater foil wrapped around the nozzle coupling spool. The result is a difference of about 2K between the cooler spool and the nozzle holder, due to a 2W heater load on the latter.

The time response of both the temperature and the pressure control has been designed to be around 10 sec. Other parameters, which have an effect on the interaction rate such as the beam current, vary with the time scale of hours. The noise is insignificant.

Given this kind of control, it is possible to maintain the density to within 20%.

Measurements of the Density and Flow of Background Gas.

To determine the jet density, the three parameters which are in the following formula have been independently measured.

$$\rho = \frac{\Phi_{Jet}}{A_{jet} \cdot V_{Cl}} \quad (3.1)$$

The cross sectional area of the jet in the interaction region depends only on the geometry of the skimmer system. The conical shape of the jet is defined by the aperture of the skimmer between chambers J2 and J3 (Fig. 6) and from the distance of the latter to the nozzle. A direct measurement of this area has been made by passing a needle through the jet. The clusters which strike the needle at room temperature evaporate completely. Using an ion gauge, it is possible to record the consequent pressure increase in the interaction region and to therefore define the spatial width of the jet. Due to the “L” shape of the needle used, the area has been measured both horizontally and vertically, verifying that its shape is indeed circular. It has also been shown that the jet shape does not vary by changing the nozzle temperature and pressure (Fig. 7).

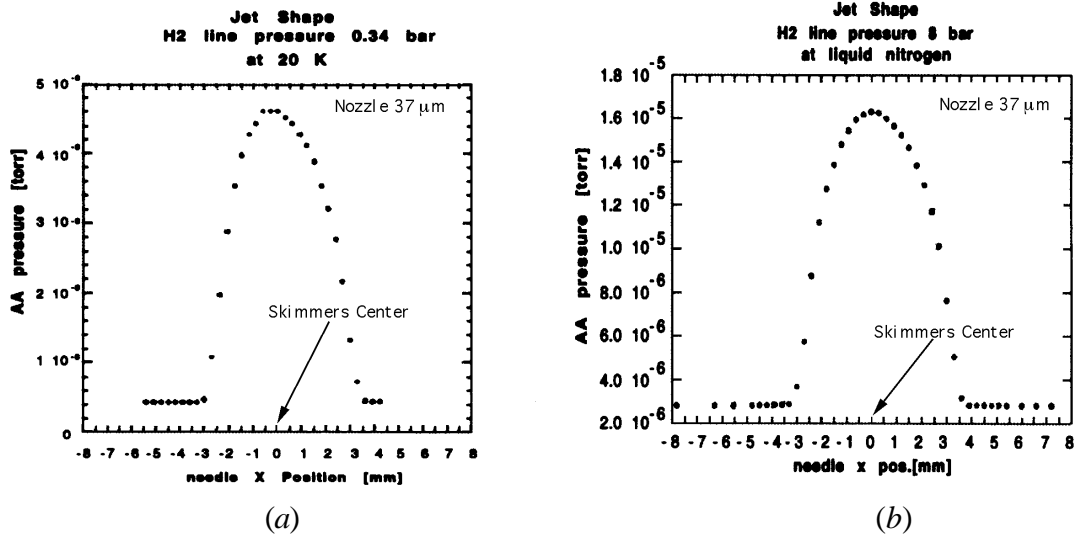


Fig. 7: Density distribution of the jet in the region of intersection with the antiproton beam. a) shape at 20K, 0.34 bar; b) shape at 77K, 8 bar.

The value obtained for this area is $A_{\text{jet}} = (3.9 \pm 0.5) \cdot 10^{-5} \text{ m}^2$ (diameter $\sim 7 \text{ mm}$). The flow Φ_{Jet} has been determined using the equation:

$$\Phi_{\text{Jet}} = \frac{S \cdot P}{R \cdot T} \quad (3.2)$$

The pressure, P , is measured inside chamber R1 as this is where the cluster jet is destroyed; the pumping speed, S , has been previously determined; T is room temperature; and, R is the universal gas constant. The pumping speed in R1, as in each chamber, has been measured by the use of a calibrated hydrogen flow (see Table 1), using again equation 3.2.

An independent measurement of the flow has been done by integrating the distributions in Fig. 7. The two measurements are consistent within the experimental errors.

The cluster speed has been measured by determining the time of flight from the interaction area to R1. This length (basis of the measurement) is 850 mm. The instrument used was a chopper installed on the jet. Using a lock-in amplifier, the phase difference between the modulate signal in R1 and a trigger has been measured for different values of the chopper frequency revolution.

The time of flight t_{of} is given by:

$$t_{\text{of}} = \frac{1}{2} \frac{1}{360} \frac{d(\Delta\Phi)}{df}$$

where $\Delta\Phi$ is the phase difference and f is the revolution frequency of the chopper.

Figure 8 shows the typical trend of the cluster speed for a constant nozzle temperature, changing the pressure. It is possible to see that, at $T=30\text{K}$, for values of the pressure greater than 20 psia, the speed saturates.

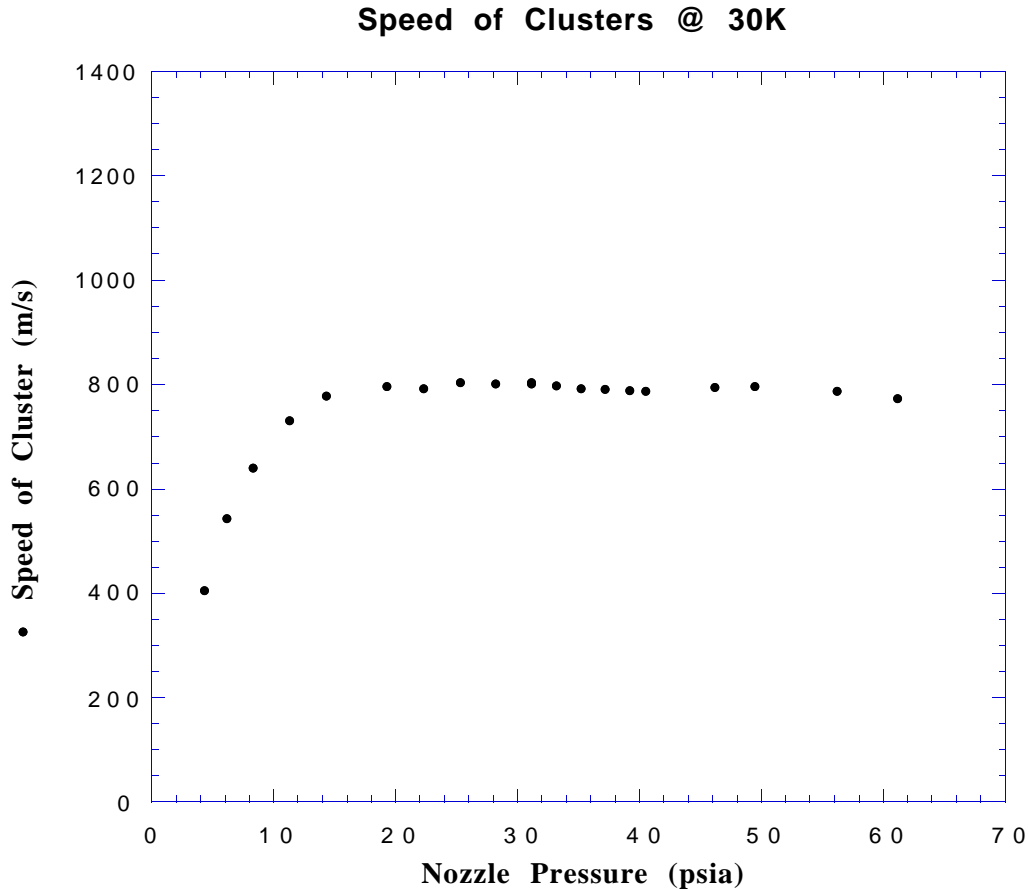


Fig. 8: The cluster speed at 30K, varying the nozzle pressure. For pressure higher than 20 psia the speed distribution saturates.

It is possible to compare these results with the value given from the Kinetic Theory:

$$V_{Cl} = \sqrt{\frac{2R}{W} \left(\frac{\gamma}{\gamma-1} \right) T}$$

where $W = 2.016 \cdot 10^{-3} \text{ Kg/mole}$, T is the nozzle temperature, R is the universal gas constant and $\gamma = c_p/c_v$ (for molecular hydrogen at low temperature equal to $5/3$). Fig. 9 shows the results.

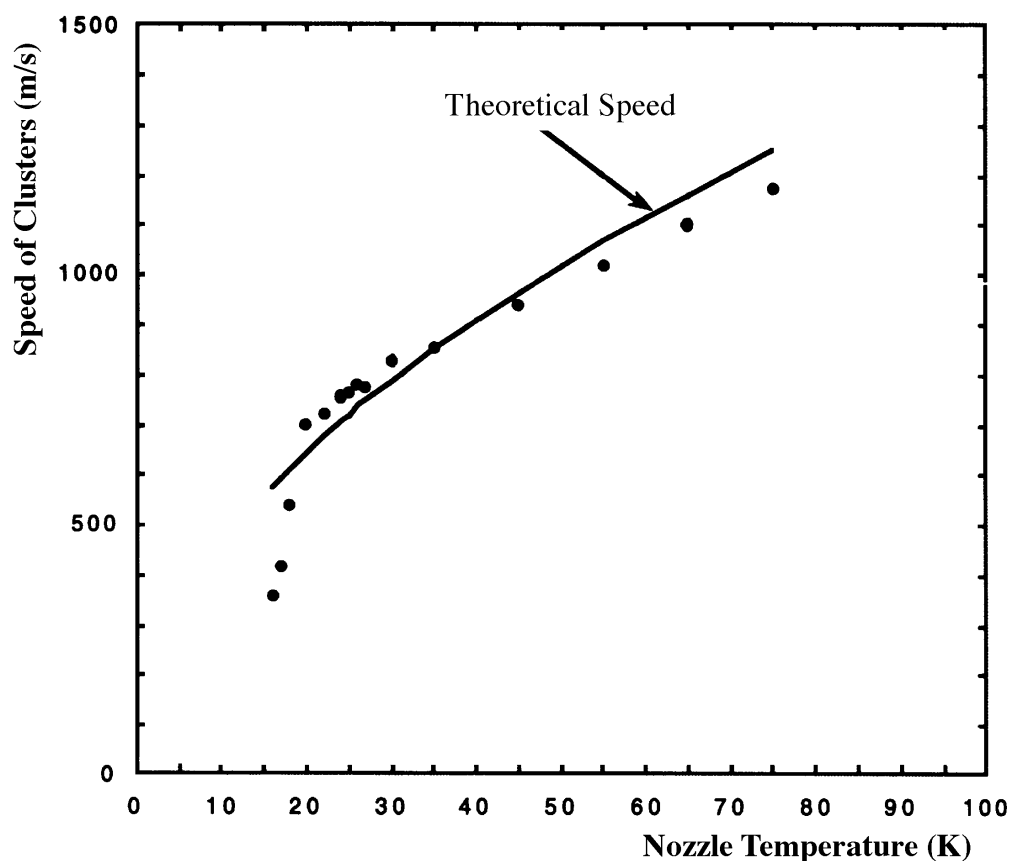


Fig. 9: Results from the cluster speed measurements. The continuous line shows the values given by the kinetic theory.

For temperatures lower than 20K, the experimental points are very different from the theoretical trend because the pressure at which the hydrogen passes from gas to liquid is lower than the pressure for observing the speed saturation. For these values of the temperature, Fig. 9 shows the maximum speed measured. The upper limit in the width of the speed distribution has been estimated at $\pm 10\%$.

Using formula 3.1, the jet density and background gas in AA have been plotted for various pressures. Fig 10 shows one of these plots at a constant temperature of 25K. Notice the trend of the curves. In choosing operating points for the jet target, pressures and temperatures resulting in the characteristic peaks are preferred.

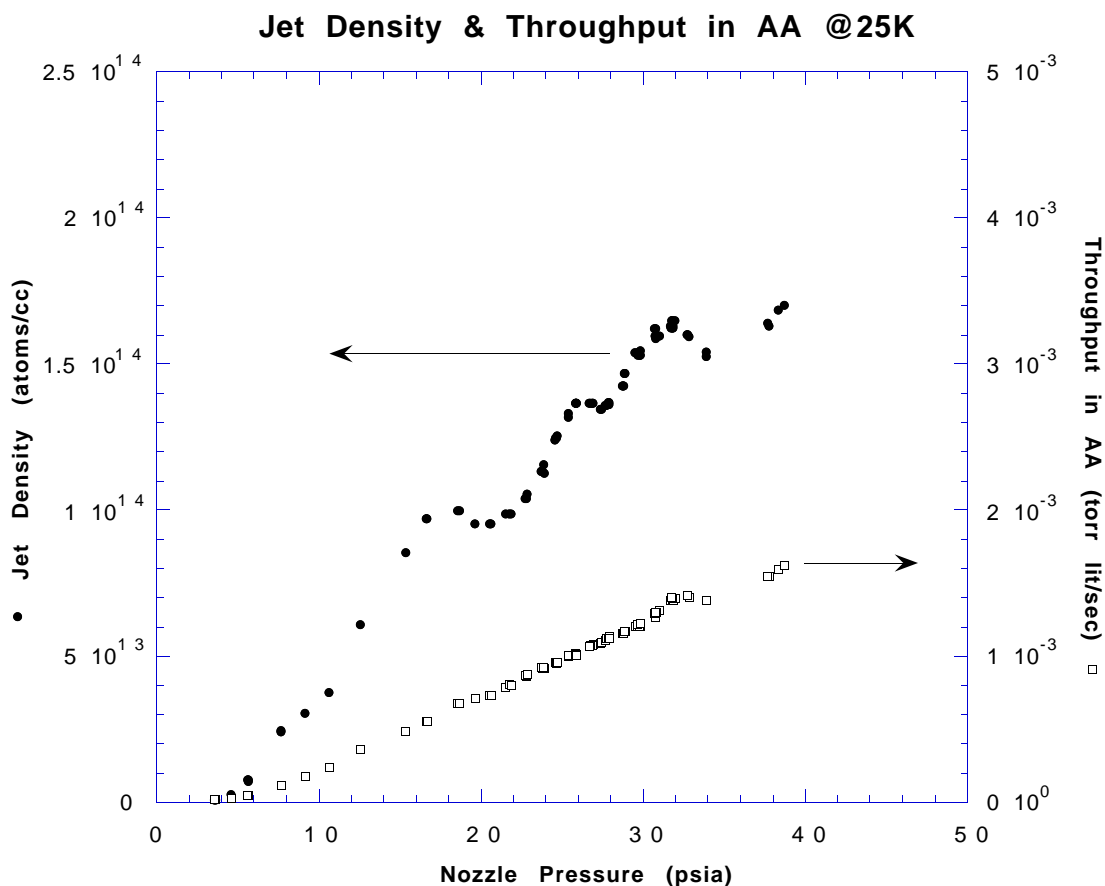


Fig. 10: Jet Density at a nozzle temperature of 25K. Also shown is the throughput of the background gas diffused in the Antiproton Accumulator.

Changing the nozzle pressure and temperature according with the trend described in Section 2, it is possible to achieve densities from $1 \cdot 10^{13}$ atoms/cc to $3.2 \cdot 10^{14}$ atoms/cc. This is more than a factor of 5 higher than the maximum density reached in E760 ($6 \cdot 10^{13}$ atoms/cc).

Considering the width of the density distribution (Fig. 7), it is possible to plot the density distribution in atoms/cm² (Fig. 11).

Density Shape in the interaction area @ 5psia, 20K

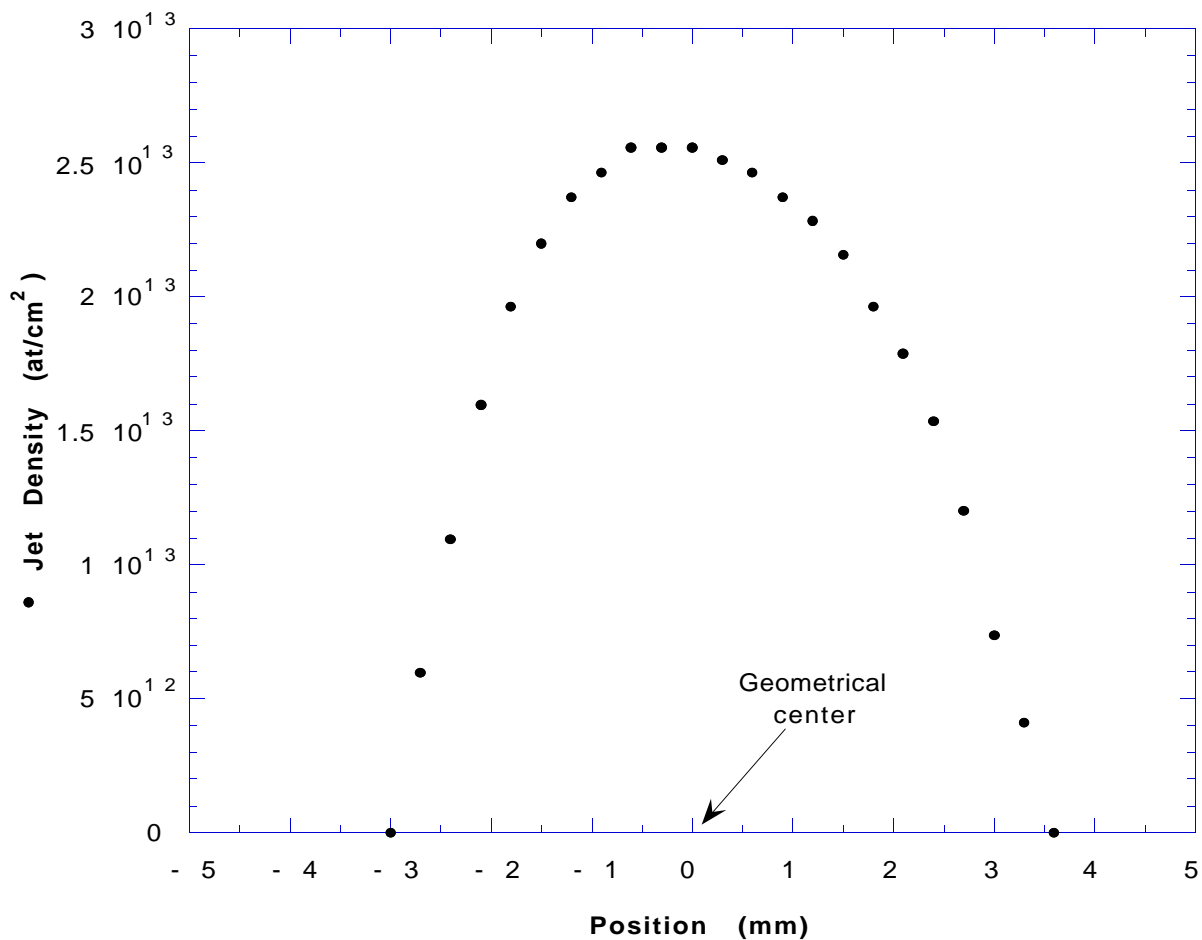


Fig. 11: The density in atoms/cm² in the interaction region with the antiproton beam. On the x axis, 0 represent the theoretical axis of the jet.

Fig. 12 shows the nozzle temperature and pressure chosen and the corresponding density values. These conditions have been reproducible throughout the last 9 months of running.

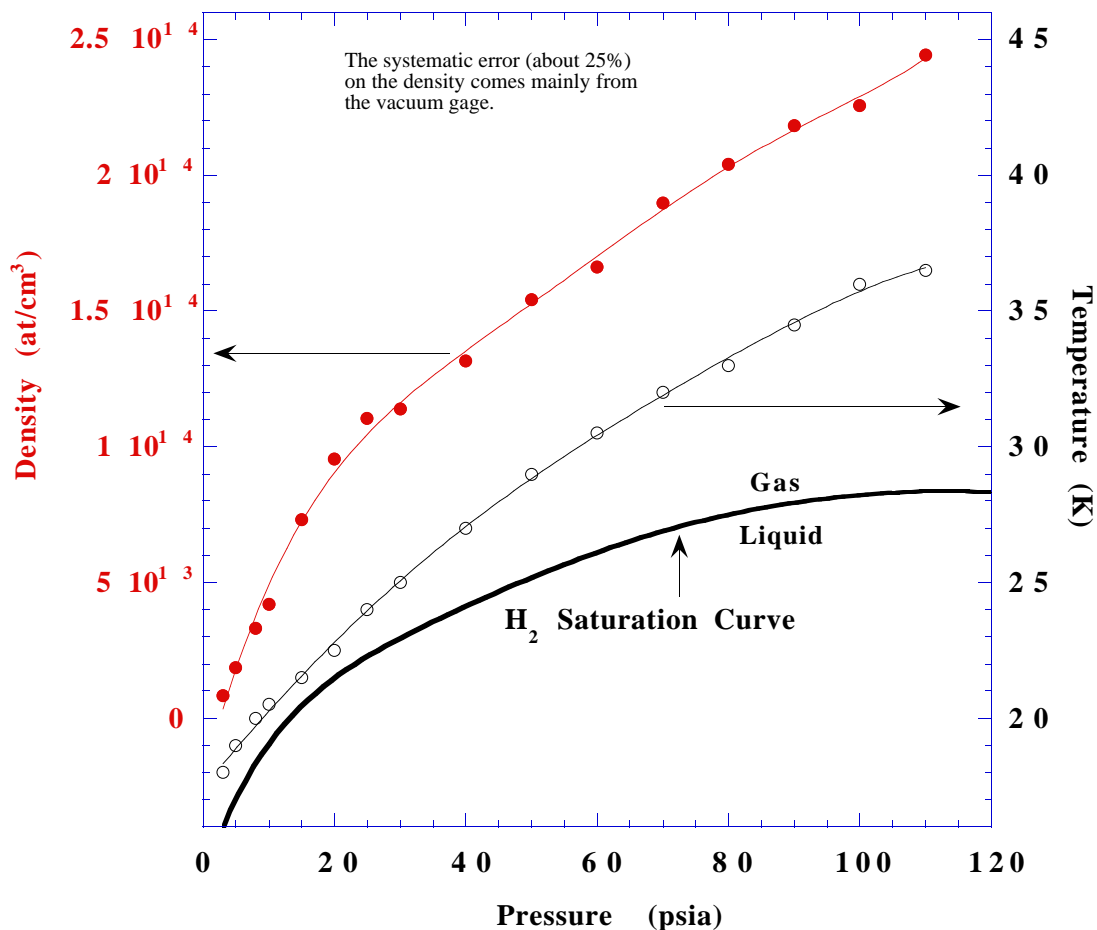


Fig. 12 The “open circle” curve (right axis) shows the Temperature vs. Pressure condition of the nozzle chosen for varying density. The “full circle” (left axis) curve shows the Density vs. Pressure obtained for that pressure and temperature. The thick black line is the saturation curve for hydrogen.

From the pressure inside the Antiproton Accumulator we know that the diffused gas along the entire length is about 5% of the gas which constitutes the target. In other words, 95% of the interactions occur in the interaction area monitored by the final state detector. This is a great improvement as compared to E760 for which the diffused gas percentage of 40%.

Adjusting the temperature and pressure according to the conditions shown in Fig. 12, it is possible to keep the instantaneous luminosity of the experiment at a constant value, typically $2 \cdot 10^{31} \text{ cm}^{-2} \text{ s}^{-1}$ (Fig. 13).

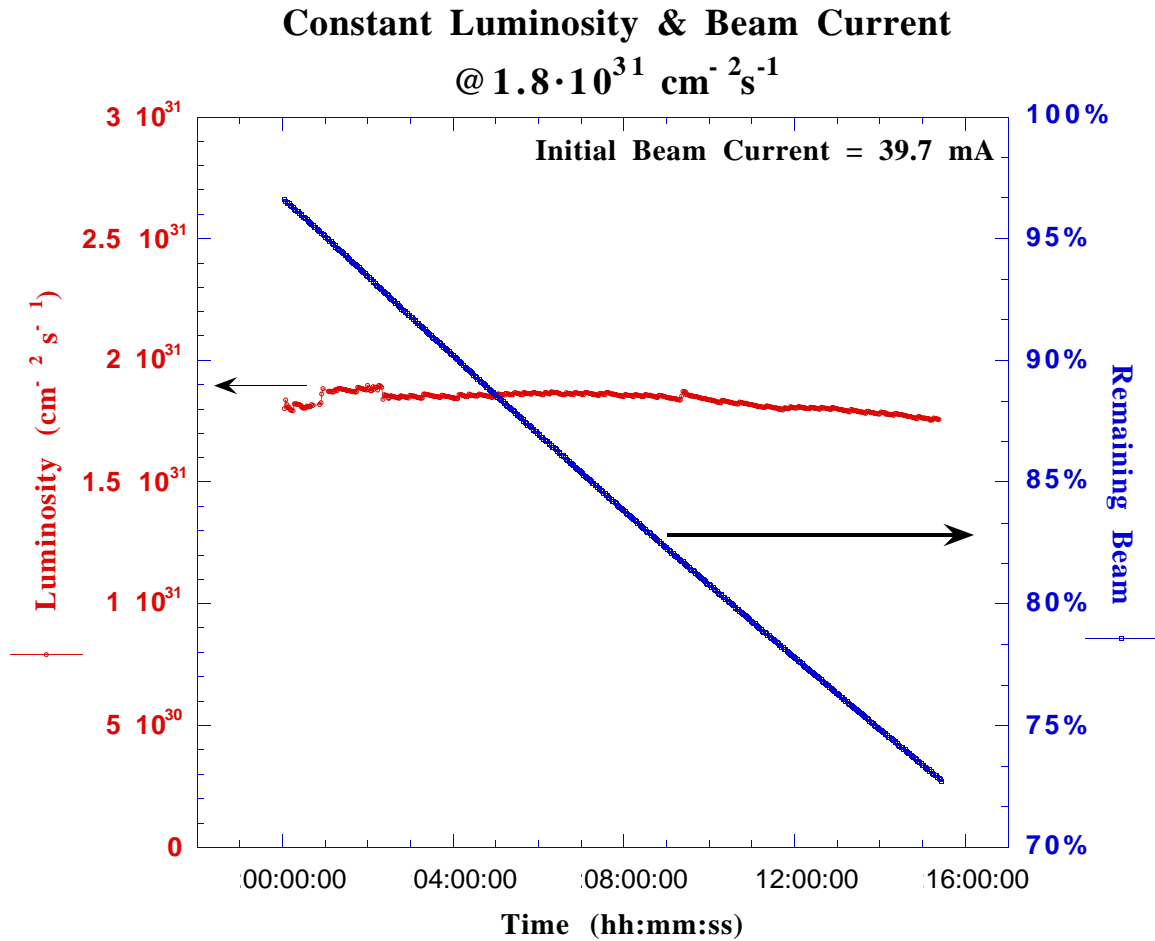


Fig. 13: A 16 hour period of data taking in which the instantaneous luminosity is kept at about $2 \cdot 10^{31} \text{ cm}^{-2} \text{ s}^{-1}$. The antiproton beam current varies from 39.7 mA to 29 mA.

4. Conclusions

The internal Gas Jet Target for E835 (Charmonium spectroscopy) at the Fermilab Antiproton Accumulator is an upgraded version of the system used in E760. Its main feature is the cryocooler expansion stage, which allows much higher densities ($3.2 \cdot 10^{14}$ atoms/cc), and a better pumping system which, together with the new alignment system, lowers the background gas. Using the Target in a new operational mode, the variable density, we have obtained a substantial increase in the integrated luminosity of the experiment.

5. Acknowledgments

The work which has made possible the achievements in the target performances is the result of a splendid collaboration between two Fermilab groups: the PAB support group (in particular R. Davis, D. Miller) and the Cryogenic group (in particular the staff of Lab 3) and the INFN technical services; the mechanical workshop (in particular F. Conforti, G. Franzone, P. Pollovio and E. Vigo), the mechanical project service (in particular G. Massari) and E. Bozzo. We would like to acknowledge the work of all the people that made possible the construction and use of the first version of the target used in Experiment 760.

-
- [1] M. Macri', *Gas Jet Targets*, CERN 84-15 (1984)
M. Macri', in *Internal Gas Jet Targets for Nuclear and Particle Physics Experiments in Hadronic Physics at Intermediate Energies*, T. Bressani Editor, Elsevier Sc. Pub. (1987)
 - [2] C. Baglin et al., *Nucl. Phys.* B286:85 (1987)
 - [3] L. Bertolotto et al., *Phys. Lett.* B345:325 91995)
 - [4] G. Baur et al., *Phys. Lett.* B368:251 (1996)
 - [5] R. Cester and P. A. Rapids, *Annu. Rev. Nucl. Part. Sci.* 44 (1994), 329
 - [6] T. A. Armstrong et al., Fermilab Proposal 835 (1992)
 - [7] O. F. Hagena, W. Obert, *J. Chem. Phys.* 59:1793 (1972)
J. Gspann, K. Korting, *J. Chem. Phys.* 59:4726 (1973)
 - [8] D. R. Miller, *Free jet sources*, in *Atomic and molecular beam methods*, vol. I, p. 14, G. Scoles ed., Oxford Univ. Press (1988)
M. Kappes, S. Leutwyler, *Molecular beams of clusters*, in *Atomic and molecular beam methods*, vol. I, p. 380, G. Scoles ed., Oxford Univ. Press (1988)
 - [9] D. H. Allspach et al., *The E760 Jet Target: measurements of performance at 77K*, Fermilab-TM-1915, Nov. 1994
 - [10] D. H. Allspach et al., *Refrigerated Hydrogen Gas Jet for the Fermilab Antiproton Accumulator*, in *Advances in Cryogenic Engineering*, vol. 41, p. 685, P. Kittel ed., Plenum Press, NY (1996)